doi:10.1093/brain/awt152 Brain 2013: 136; 2120–2129 | 2120

BRAIN
A JOURNAL OF NEUROLOGY

The coeruleus/subcoeruleus complex in rapid eye movement sleep behaviour disorders in Parkinson's disease

Daniel García-Lorenzo,[1,2] Clarisse Longo-Dos Santos,[3,4] Claire Ewenczyk,[2,5] Smaranda Leu-Semenescu,[2,6] Cecile Gallea,[1,2] Graziella Quattrocchi,[2,5] Patricia Pita Lobo,[2,5] Cyril Poupon,[3,4] Habib Benali,[4,7] Isabelle Arnulf,[2,6] Marie Vidailhet[2,5,*] and Stéphane Lehericy[1,2,4,8,*]

1 Institut du Cerveau et de la Moelle épinière, Centre de Neuroimagerie de Recherche, Paris, France
2 Université Pierre et Marie Curie (UPMC Univ Paris 6), Centre de Recherche de l'Institut du Cerveau et de la Moelle epiniere, UMR-S975; Inserm, U975; CNRS, UMR 7225, Paris, France
3 CEA, NeuroSpin, 91191 Gif-Sur-Yvette, France
4 IFR49 Institut d'Imagerie Neurofonctionnelle, CEA/SAC/DSV/I2BM/NeuroSpin, France
5 Federation de Neurologie, Groupe Hospitalier Pitié-Salpêtrière, Paris, France
6 Service des pathologies du sommeil, Groupe Hospitalier Pitié-Salpêtrière, Paris, France
7 Inserm U678, Laboratoire d'Imagerie Fonctionnelle, Paris, France
8 Service de neuroradiologie, Groupe Hospitalier Pitié-Salpêtrière, Paris, France

*These authors contributed equally to this work.

Correspondence to: Stéphane Lehericy, M.D., Ph.D.,
CENIR ICM, Groupe Hospitalier Pitié-Salpêtrière,
75651 Paris, cedex 13 France
E-mail: stephane.lehericy@psl.ap-hop-paris.fr

In Parkinson's disease, rapid eye movement sleep behaviour disorder is an early non-dopaminergic syndrome with nocturnal violence and increased muscle tone during rapid eye movement sleep that can precede Parkinsonism by several years. The neuronal origin of rapid eye movement sleep behaviour disorder in Parkinson's disease is not precisely known; however, the locus subcoeruleus in the brainstem has been implicated as this structure blocks muscle tone during normal rapid eye movement sleep in animal models and can be damaged in Parkinson's disease. Here, we studied the integrity of the locus coeruleus/subcoeruleus complex in patients with Parkinson's disease using combined neuromelanin-sensitive, structural and diffusion magnetic resonance imaging approaches. We compared 24 patients with Parkinson's disease and rapid eye movement sleep behaviour disorder, 12 patients without rapid eye movement sleep behaviour disorder and 19 age- and gender-matched healthy volunteers. All subjects underwent clinical examination and characterization of rapid eye movement sleep using video-polysomnography and multimodal imaging at 3 T. Using neuromelanin-sensitive imaging, reduced signal intensity was evident in the locus coeruleus/subcoeruleus area in patients with Parkinson's disease that was more marked in patients with than those without rapid eye movement sleep behaviour disorder. Reduced signal intensity correlated with the percentage of abnormally increased muscle tone during rapid eye movement sleep. The results confirmed that this complex is affected in Parkinson's disease and showed a gradual relationship between damage to this structure, presumably the locus subcoeruleus, and abnormal muscle tone during rapid eye movement sleep, which is the cardinal marker of rapid eye movement sleep behaviour disorder. In longitudinal studies, the technique may also provide early markers of non-dopaminergic Parkinson's disease pathology to predict the occurrence of Parkinson's disease.

Received February 28, 2013. Revised April 23, 2013. Accepted April 29, 2013

Keywords: MRI; RBD; diffusion imaging; neuromelanin-sensitive imaging; VBM
Abbreviation: RBD = rapid eye movement sleep behaviour disorder

Introduction

In recent years, research has been focused on the identification and quantification of non-dopaminergic lesions of the brainstem in Parkinson's disease in light of Braak's neuropathological staging (Braak *et al*., 2003, 2004). In particular, non-motor signs such as rapid eye movement (REM) sleep behaviour disorder (RBD) have received particular attention. RBD is characterized by prominent motor activity accompanying dreaming associated with the loss of normal skeletal muscle atonia that occurs during REM sleep (Schenck and Mahowald, 2002; Iranzo and Aparicio, 2009). RBD may appear in subjects without any other neurological disease (idiopathic RBD). Patients with idiopathic RBD have increased risk of developing Parkinson's disease, dementia with Lewy bodies and, more rarely, multiple system atrophy, with a rate of conversion of ~50% within 5 years (Iranzo *et al*., 2006; Boeve *et al*., 2007; Postuma *et al*., 2009). In Parkinson's disease, RBD affects 30–60% of patients (De Cock *et al*., 2007). In patients with Parkinson's disease, RBD is associated with older age, longer disease duration, decreased cognitive performances and hallucinations, and therefore worse prognosis (Arnulf, 2012).

In animal models, RBD was observed after selective damage in the pontine tegmentum, encompassing the locus coeruleus perialpha in cats (Sastre and Jouvet, 1979) and the sublaterodorsalis nucleus in rats (Lu *et al*., 2006). These nuclei are equivalent to the locus subcoeruleus in humans. In humans, rare cases of lesions in the pontine and midbrain tegmentum resulting in RBD were reported (Boeve *et al*., 2007; Iranzo and Aparicio, 2009). A patient with Parkinson's disease and RBD had numerous alpha-synuclein deposits within the locus coreuleus/subcoeruleus melanized cells on brain examination (Arnulf *et al*., 2000). Among these nuclei, the locus subcoeruleus is particularly involved in the control of atonia during REM sleep (Lu *et al*., 2006; Boeve *et al*., 2007).

Recently, MRI has been used to investigate the structural changes associated with RBD. Diffusion changes using MRI were localized in the midbrain tegmentum, rostral pons and pontine reticular formation in patients with idiopathic RBD (Scherfler *et al*., 2010), whereas changes were found in the brainstem, substantia nigra, olfactory regions and other brain regions in another study (Unger *et al*., 2010). The locus coeruleus/subcoeruleus complex contains catecholaminergic neurons that contain a pigment, neuromelanin (Baker *et al*., 1989). When combined with metals such as iron and copper, neuromelanin has paramagnetic T_1-shortening effects (Bazelon *et al*., 1967; Enochs *et al*., 1997) and displays bright signal intensity in healthy human subjects (Keren *et al*., 2009). In patients with Parkinson's disease, decreased signal intensity was detected in the locus coeruleus/subcoeruleus area (Sasaki *et al*., 2006; Shibata *et al*., 2006) that was interpreted as reflecting a loss of neuromelanin-containing neurons, but no correlations were performed with abnormal sleep.

Here, we studied the locus coeruleus/subcoeruleus complex using combined neuromelanin-sensitive structural and diffusion MRI approaches in patients with Parkinson's disease with and without RBD and correlated imaging changes with clinical characterization of RBD and enhanced muscle tone in REM sleep using video-polysomnography. We confirm that structural changes can be detected in the locus coeruleus/subcoeruleus in Parkinson's disease and that these changes specifically correlate with abnormally increased muscle tone during REM sleep.

Materials and methods

Subjects

Forty-one patients were prospectively recruited in the Movement Disorders clinic of the Pitie-Salpetriere Hospital, between April 2010 and September 2012. Patients had to meet the following inclusion criteria: clinical diagnosis of idiopathic Parkinson's disease (according to the UK Parkinson's disease brain bank criteria), age between 18 and 75 years, no or minimal cognitive disturbances (Mini-Mental State Examination > 24). For comparison, 22 normal healthy volunteers with no history of neurological disorders were also recruited. Healthy volunteers were matched for age and gender. All subjects gave written informed consent and the study was approved by the local ethics committee.

Neurological examination

A complete neurological examination was performed and the severity of extrapyramidal symptoms was quantified using the Unified Parkinson's disease Rating Scale part III and the Hoehn and Yahr stage. DOPA sensibility was assessed by an acute levodopa challenge after overnight withdrawal of dopaminergic treatments. The L-DOPA dose corresponded to the usual morning levodopa equivalent dose + 50 mg. Cognitive impairment was assessed using the Mini-Mental State Examination (Folstein *et al*., 1975).

The presence of RBD was assessed as follows. Subjects were interviewed about their sleeping habits during the current year by experienced sleep neurologists (I.A. and S.L.S.) using a semi-structured questionnaire that was adapted from an RBD questionnaire (Comella *et al*., 1998). The patients and their bed partners when available were separately interviewed about RBD in the presence of one another. Clinical RBD was defined when the bed partner reported significant, purposeful limb or body movements during sleep (as if patients were acting out their dreams) and when these movements were associated with a dream recall when the patient was awake. This questionnaire has been validated previously (De Cock *et al*., 2007). When confronted with objective video-polysomnography criteria of RBD, the accuracy of the questionnaire in detecting RBD in patients with Parkinson's disease reached 97% sensitivity (De Cock *et al*., 2011).

Sleep monitoring

Sleep and nocturnal movements were monitored during a single night for all subjects. The monitoring included Fp1-Cz, O2-Cz and C3-A2 EEG; right and left electrooculogram; nasal pressure monitoring through a cannula; tracheal sounds through a microphone; thoracic

and abdominal belts for assessing respiratory efforts; electrocardiography; pulse oximetry; EEG-synchronized infra-red video monitoring and an ambiance microphone. The electromyography (EMG) recording of the levator menti, and right and left tibialis anterior muscles was monitored. The sleep stages, arousals, respiratory events, periodic leg movements and muscle activities were scored through visual inspection according to standard criteria (Iber *et al*., 2007).

Video and electromyography movement analysis

We determined the presence or absence of RBD in this group of patients through interviews, video and sleep monitoring using international criteria (Iber *et al*., 2007). Alternatively, if no motor behaviour was observed in the video, we required the presence of REM sleep without atonia (defined as the time containing REM sleep epochs with at least 50% of the duration of the epoch having a chin EMG amplitude greater than the minimum amplitude in non-REM sleep muscle tone divided by total REM sleep time) lasting >30% of the REM sleep time and a history of dream enactment (Gagnon *et al*., 2002; Montplaisir *et al*., 2010). Sleep measures that were recorded included total sleep time, sleep efficiency (total sleep time divided by total sleep duration), per cent of non-REM sleep N1, N2 and N3 + 4 stages, percentage of REM sleep (duration of REM sleep divided by total sleep time), percentage of REM sleep without atonia (duration of REM sleep without atonia divided by the total duration of REM sleep).

Magnetic resonance imaging data acquisition

Magnetic resonance acquisitions were performed using a 3 T whole body TRIO 32-channel TIM system (Siemens). Radiofrequency transmission was performed with body coil, and signal was received with a 12-channel receive head coil. The protocol included whole brain high resolution anatomical 3D T_1-weighted images, neuromelanin-sensitive images (T_1-weighted), and diffusion imaging. Whole brain 3D T_1-weighted scans were acquired using a sagittal MP-RAGE acquisition (inversion time: 900 ms, repetition time/echo time/flip angle: 2300 ms/4.18 ms/9°, one average, voxel size: $1 \times 1 \times 1$ mm^3). Neuromelanin-sensitive images were acquired using 2D axial turbo spin echo T_1-weighted images (repetition time/echo time/flip angle: 900 ms/15 ms/180°, three averages, voxel size: $0.4 \times 0.4 \times 3$ mm^3). This acquisition was repeated twice using the exact same parameters. Diffusion images were acquired using echo-planar imaging (EPI) in the axial plane (repetition time/echo time/flip angle: 14 s/101 ms/90°, voxel size: $1.7 \times 1.7 \times 1.7$ mm^3, b-value: 1500 s/mm^2, 60 gradient encoding directions). Five patients and three healthy volunteers were removed from this study because of severe movement during acquisition.

Image analysis

Image analysis was performed blindly to the clinical status of the patients.

Neuromelanin-sensitive images

Each neuromelanin-sensitive T_1-weighted image was processed independently. The majority of subjects moved slightly between the two neuromelanin-sensitive acquisitions, preventing us directly averaging voxel-by-voxel both acquisitions to increase the signal-to-noise ratio (SNR). Due to the small size of the locus coeruleus and the anisotropic voxel size of the images, we decided not to register both images to avoid interpolation artefacts. The anatomical whole brain 3D T_1-weighted images were corrected for intensity inhomogeneity (Sled *et al*., 1998) and a non-linear transformation towards the new high resolution ICBM template (Fonov *et al*., 2011) was calculated using a non-linear registration algorithm (Avants *et al*., 2008). Each neuromelanin-sensitive T_1-weighted image was rigidly registered to the 3D T_1-weighted volume.

To calculate the signal intensity in the locus area, three regions (serving as bounding boxes) were manually defined on the ICBM template (Fig. 1). Combining rigid and non-linear transformations, the three regions were resampled onto the neuromelanin-sensitive T_1-weighted images.

The first region was defined in the rostral pontomesencephalic area (6200 mm^3) and was used as a reference region to normalize the intensity of the slices to remove the inter-slice and inter-subject variability. For each slice, the intensity of the slice was linearly modified so that the average intensity of this region was set to the same arbitrary value in all the images. This normalization allowed the direct comparison of intensity values between subjects. The other two regions (one for each side, 700 mm^3) were defined as large 3D bounding boxes so as to include the locus coeruleus/subcoeruleus complex, but to avoid any other structure that could be considered as 'bright' in the neuromelanin-sensitive T_1-weighted images, such as the substantia nigra which also contains neuromelanin. These bounding box regions were resampled from the template onto the subject (Fig. 1). We then considered that the brightest voxels found in these 3D regions corresponded to the locus area. To avoid errors caused by noise, the locus was defined within this bounding box as the area of 10-connected voxels with the brightest intensity that were automatically found using in-house developed software. The 10-voxel size of the locus area was chosen to be large enough to avoid errors due to noise and to provide a good estimate of the intensity of the locus but was smaller than its actual size. We considered the intensity of the locus as the average of the intensities of the 10-connected voxel region. The bounding box was used to avoid software detection of the maximum intensity outside the area of the locus coeruleus/subcoeruleus complex in subjects with low signal intensity and therefore restricted the search to this area.

Voxel-based morphometry

From the 3D T_1-weighted volume, we obtained the normalized and modulated grey matter and white matter probability maps using the VBM8 toolbox (http://dbm.neuro.uni-jena.de/vbm/) in the SPM8 software (http://www.fil.ion.ucl.ac.uk/spm/) running on MATLAB R2010b (The MathWorks, Inc.). The processing included de-noising (Manjon *et al*., 2010), partial volume estimation (Tohka *et al*., 2004) and normalization to the MNI space using DARTEL (Ashburner and Friston, 2005) and the software template based on 550 healthy control subjects. The normalized maps were smoothed with 4 mm full-width at half-maximum Gaussian kernel.

Voxel-based diffusion imaging

Diffusion images were processed using BrainVISA/Connectomist-2.0 diffusion toolbox to correct for eddy currents, susceptibility deformations and patient movements (Duclap *et al*., 2012). Then the fractional anisotropy and apparent diffusion coefficient images were computed. The fractional anisotropy maps were non-linearly registered to a fractional anisotropy template using FNIRT

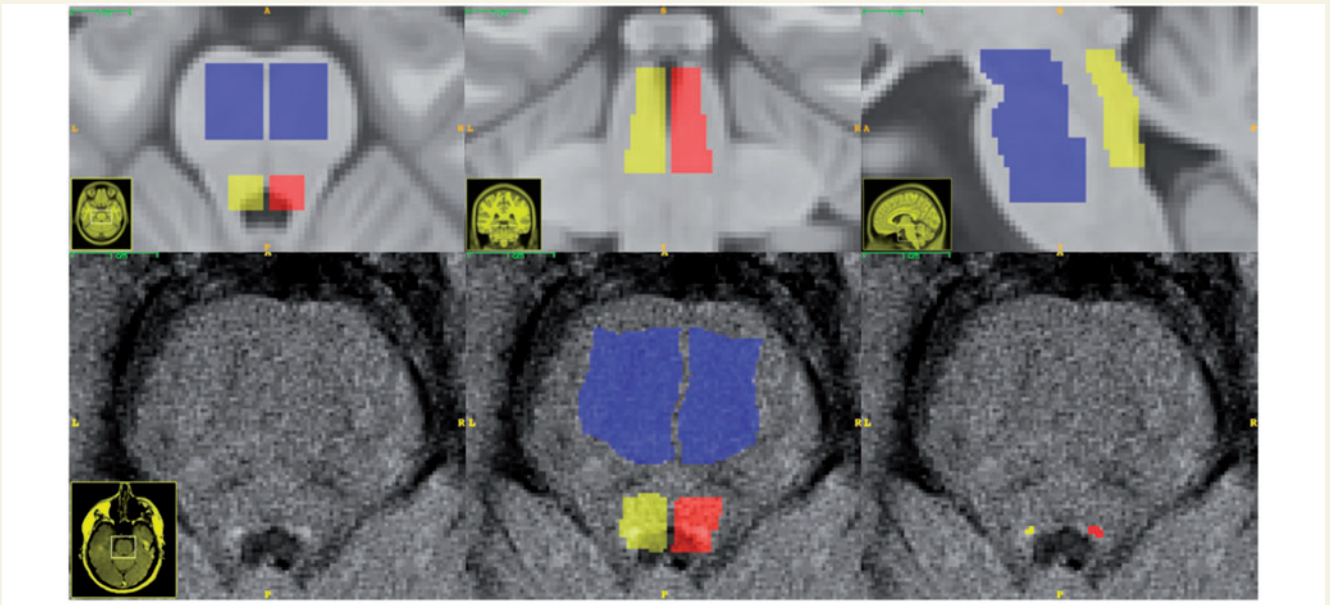

Figure 1 Definition of the locus coeruleus/subcoeruleus area using the template regions. (*Top*) ICBM template regions: bounding box regions were manually defined on the ICBM template in the ponto-mesencephalic area (blue, used for signal normalization), the left (red) and right (yellow) locus areas. Regions are represented in the axial (*left*), coronal (*middle*) and sagittal plane (*right*). (*Bottom left*) Axial 2D neuromelanin-sensitive T_1-weighted image in a representative healthy volunteer passing at the level of the locus area. (*Middle*) Template regions were resampled onto the individual images using combined rigid and non-linear transformations. (*Right*) Voxels of maximum signal intensity in the left (red) and right (yellow) locus area.

(Jenkinson *et al.*, 2011). The same deformation fields were applied to the apparent diffusion coefficient maps. No modulation was applied. The normalized fractional anisotropy and apparent diffusion coefficient were smoothed with a 4 mm full-width at half-maximum Gaussian kernel.

Statistical analysis

Statistical analyses of the locus intensities and the clinical metrics were performed using Matlab. Reproducibility of signal measurements in the coeruleus/subcoeruleus complex was evaluated using paired Wilcoxon signed rank test. The three groups of subjects (healthy volunteers, patients with RBD and patients without RBD) were compared using a non-parametric Kruskal-Wallis test corrected for multiple comparisons using Tukey's honestly significant difference criterion. Non-parametric tests were chosen because of the non-Gaussian distribution of signal intensities in the patients. The correlation analysis between signal intensity in the coeruleus/subcoeruleus complex and the clinical variables was performed using Spearman correlation correcting for age and gender. The level of statistical significance was set to $P < 0.05$.

Voxel-based analyses were performed using SPM8. ANOVA was used to compare RBD patients, non-RBD patients and healthy volunteers using gender and age as covariates in grey matter, white matter, fractional anisotropy and apparent diffusion coefficient maps. Analyses were limited to the brainstem using the brainstem atlas mask of SMP8 (for grey and white matter) or FSL (for fractional anisotropy and apparent diffusion coefficient maps). Maps were thresholded at $P < 0.001$ at the voxel level uncorrected for multiple comparisons. Clusters were then considered significant at $P < 0.05$ corrected for multiple comparisons. Uncorrected results are presented as trends.

The accuracy of neuromelanin-sensitive images to classify patients with and without RBD was also evaluated by using a k-nearest neighbour algorithm (k = 3) with the signal intensity of the coeruleus/subcoeruleus complex as input. To validate the approach, 100 random experiments were performed where 12 RBD patients were randomly chosen to match the number of non-RBD patients. For each experiment, a leave-one-out cross validation was employed where each patient was classified using the 23 other patients as training points.

Results

Clinical and sleep characteristics of subjects

The clinical characteristics of the patients and healthy volunteers are summarized in Table 1. Thirty-six patients with Parkinson's disease (41 initially recruited, five were excluded for head motion during MRI acquisition) and 19 healthy volunteers (22 initially recruited, three were excluded for head motion) matched for age and gender with no history of neurological disorders were included in the statistical analyses. The group of 36 patients included 24 patients with RBD and 12 patients without RBD. Patient groups did not differ for disease duration, motor disability and performances at the Mini-Mental State Examination. For sleep tests, patients with RBD showed reduced sleep efficiency compared with healthy volunteers and increased percentage of REM sleep without atonia as compared with both healthy volunteers and patients without RBD. There was no other significant comparison.

Table 1 Clinical characteristics of the subjects

	Healthy volunteers	All patients	RBD	Without RBD
n	19	36	24	12
Sex ratio (M/F)	10/9	23/13	16/8	6/6
Age (years)	60.2 ± 8.3	60.3 ± 9.8	62.4 ± 8.4	56.3 ± 11.5
Most affected side (L/R/data absent)		18/16/2	13/10/1	5/6/1
Disease duration (years)	NA	9.6 ± 4.0	9.6 + 3.8	9.7 ± 4.5
Clinical tests				
Motor disability[a] OFF DOPA		29.5 ± 9.0	30.3 ± 9.4	27.4 ± 8.4
Motor disability ON DOPA	NA	16.1 ± 9.3	17.5 ± 9.1	12.6 ± 7.0
Response to L-DOPA (%)	NA	48.4 ± 20.1	43.5 ± 19.0	55.4 ± 18.1
Mini-Mental State Examination score	28.7 ± 1.1	28.1 ± 1.7	28.1 + 1.9	28.5 ± 0.8
Sleep tests				
Total sleep time (min)	436 ± 86	356 ± 93	375 ± 80	341 ± 118
Sleep efficiency (%)	86.2 ± 6.1	76.5 ± 11.2	77.0 ± 9.9*	80.2 ± 8.8
N1 sleep (% of total sleep time)	6.1 ± 2.6	9.0 ± 12.9	7.1 ± 4.2	12.7 ± 22.9
N2 sleep (% of total sleep time)	51.1 ± 6.3	54 ± 9.7	51.1 ± 9.1	57.5 ± 10.7
N3 sleep (% of total sleep time)	9.8 ± 5.1	9.9 ± 7.6	11.9 ± 9.0	8.9 ± 5.3
REM sleep (% of total sleep time)	19.0 ± 5.0	20.0 ± 7.0	20.7 ± 6.2	17.5 ± 5.6
REM sleep without atonia (% of REM sleep)	3.4 ± 7.3	35.2 ± 37.7*	49.0 ± 34.3*	11.5 ± 28.4**

Values are means ± standard deviations.

[a]Motor disability score is the subscore 3 of the Unified Parkinson's disease Rating Scale-III; Response to L-DOPA was calculated as the ratio OFF – ON / OFF of the Unified Parkinson's disease Rating Scale III scores. All patients: all patients with Parkinson's disease with and without RBD together; RBD: patients with Parkinson's disease and RBD; without RBD: patients with Parkinson's disease and without RBD. Significance at $P < 0.05$, *indicates a difference with healthy volunteers and **with patients without RBD.

Magnetic resonance imaging data analysis

Increase in signal intensity was reliably detected in neuromelanin-sensitive images of the brainstem, extending from the area of the inferior red nucleus rostrally, to the pons at the level of the superior cerebellar peduncles caudally. To evaluate the reproducibility of signal measurements in the coeruleus/subcoeruleus complex, we first compared the values of signal intensity in this complex between the two sets of neuromelanin-sensitive images obtained in each subject. There was no significant difference between the two acquisitions ($P = 0.88$) and a strong correlation between the intensities in the first and in the second scans for both left ($r = 0.75$, $P < 1 \times 10^{-10}$) and right coeruleus/subcoeruleus area ($r = 0.73$, $P < 1 \times 10^{-10}$). To reduce the variability of the measure, we averaged the values of signal intensity obtained independently from both images for the following analyses. A paired *t*-test showed a significant difference between the left and right coeruleus/subcoeruleus complex ($P < 1 \times 10^{-5}$) although a strong correlation was also found between left and right complex ($r = 0.76$, $P < 1 \times 10^{-11}$). We averaged, left and right values to increase the signal-to-noise ratio of the coeruleus/subcoeruleus complex.

Comparison of patients with RBD, without RBD and healthy volunteers showed that RBD patients presented a significant decrease in signal intensity compared with both healthy volunteers and patients without RBD (Kruskal-Wallis test corrected for multiple comparisons, $P < 0.05$, Figs 2 and 3). There was no difference in mean signal intensity between patients without RBD and healthy volunteers. No significant differences for gender or correlations with age were found regarding signal intensity in either the healthy volunteers or patients.

The correlation analysis between signal intensity in the coeruleus/subcoeruleus complex and the clinical variables in the entire patient group demonstrated significant and specific negative correlation with the percentage of REM sleep without atonia (-0.49, $P < 0.005$), even when controlled for gender and age (Table 2 and Fig. 4). This correlation was also observed in patients with RBD (-0.50, $P < 0.05$) but not in patients without RBD (Table 2 and Fig. 4). There were no other significant correlations with any sleep metrics, scores at the motor tests or Mini-Mental State Examination.

Classification of the patients with and without RBD using the signal intensity of the coeruleus/subcoeruleus complex showed an average accuracy of 71 ± 6%.

There was no significant difference in grey and white matter between patients and healthy volunteers or between subgroups of patients. Compared with healthy volunteers, patients with RBD showed significant increases in fractional anisotropy in the tegmentum of the midbrain and rostral pons in the left hemisphere in an area including the coeruleus/subcoeruleus (cluster size: 309 mm^3, MNI coordinates: −11 −37 −30, T-score: 4.43) and a trend in the right hemisphere (cluster size: 125 mm^3, coordinates: 11 −38 −30, T-score: 4.44, uncorrected for multiple comparisons) (Fig. 5). There was no difference in fractional anisotropy between subgroups of patients or between patients without RBD and healthy volunteers. Compared with healthy volunteers, patients with RBD showed significant increases in apparent diffusion coefficient in the pontine tegmentum and the midbrain in the area of the cerebral peduncles and substantia nigra in the right

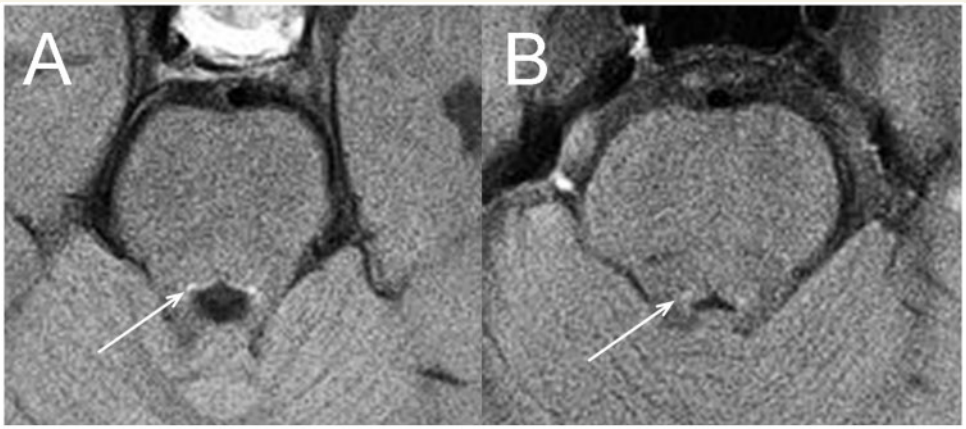

Figure 2 Neuromelanin-sensitive imaging of the locus coeruleus/subcoeruleus. Axial neuromelanin-sensitive T_1-weighted images of the locus in a healthy volunteer (**A**) and a patient with Parkinson's disease (**B**). The locus area (arrows) is visible as an area of increased signal intensity.

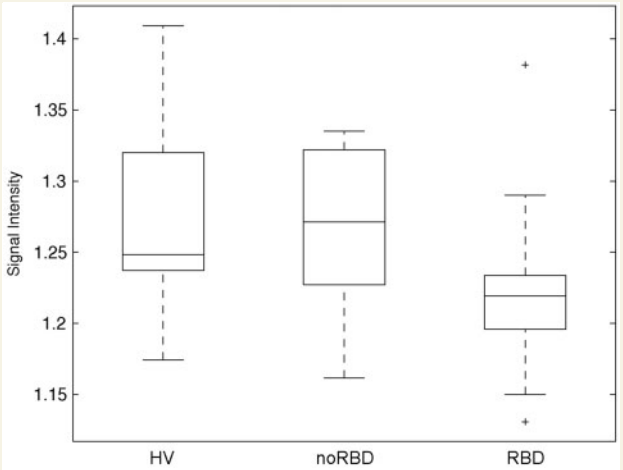

Figure 3 Box plot of the locus intensity in healthy volunteers and patients with Parkinson's disease. Signal intensity: normalized signal intensity in the locus area. Plots indicate median, the boxes indicate the upper and lower quartiles. Whiskers are defined as the lowest (highest) values still within the 1.5 interquartile range from the box. Outliers outside the 1.5 interquartile range are shown as crosses (in the RBD group). HV = healthy volunteers, noRBD = patients without RBD, RBD = patients with RBD.

hemisphere (cluster size: 575 mm^3, coordinates: 13 −21 −20, T-score: 4.43, Fig. 5) and a trend in the left hemisphere (cluster size: 337 mm^3, coordinates: −11 −16 −21, T-score: 4.77). Compared with healthy volunteers, patients without RBD showed significant increases in apparent diffusion coefficient in the same regions (cluster size: 705 and 878 mm^3, MNI coordinates: −13 −25 −35 and 8 −14 −21, T-score: 5.7 and 5.53 in the left and right hemispheres, respectively). No difference was found between patients with and without RBD. There were no significant correlations between fractional anisotropy or apparent diffusion coefficient and clinical variables.

Discussion

We showed a significant decrease in signal intensity in the locus coeruleus/subcoeruleus complex using neuromelanin-sensitive MRI techniques in patients with Parkinson's disease with versus without RBD and healthy volunteers that correlated specifically with atonia during REM sleep. Voxel-based diffusion analyses also showed significant increases in fractional anisotropy and apparent diffusion coefficient in the area of the tegmentum of the midbrain and rostral pons specifically in patients with RBD when compared with healthy volunteers.

Evidence implicating the locus subcoeruleus in the pathophysiology of REM sleep comes from animal studies as well as lesion and imaging studies in humans (Boeve *et al*., 2007). In rats, the sublaterodorsalis nucleus, equivalent to the locus subcoeruleus in humans, is the major structure responsible for REM sleep (Boissard *et al*., 2002, 2003; Lu *et al*., 2006). The sublaterodorsalis nucleus is considered as a REM-on structure e.g. that turns on REM sleep and inhibits spinal cord motor neurons resulting in atonia during REM sleep (Luppi *et al*., 2010). In humans, studies have reported that lesions within or near the midbrain and pontine tegmentum result in RBD (Kimura *et al*., 2000; Provini *et al*., 2004; Tippmann-Peikert *et al*., 2006; Limousin *et al*., 2009). More recently, changes in diffusion metrics (decrease in fractional anisotropy, increase in mean diffusivity or decrease in axial diffusivity) were reported in the tegmentum of the midbrain and rostral pons in patients with idiopathic RBD (Scherfler *et al*., 2010; Unger *et al*., 2010). In these two studies, the brainstem regions that were reported included several nuclei involved in REM sleep mechanisms such as the ventrolateral periaqueductal grey matter, the laterodorsal tegmental nucleus, the pedunculopontine nucleus and the locus coeruleus/subcoeruleus complex (Boeve *et al*., 2007). However, none of these studies used imaging techniques that allowed for more precise allocation of RBD to specific brainstem nuclei. Lesion of the locus subcoeruleus is thus hypothesized as the key nucleus involved in atonia during REM sleep, being the final

Table 2 Correlation analysis between clinical variables and signal intensity in the locus area

Examination	Parkinson's disease	RBD	Without RBD
Motor and cognitive tests			
Motor disability score OFF	−0.12 (0.02)	0.17 (0.18)	−0.22 (−0.14)
Response to L-DOPA (%)	0.15 (−0.01)	−0.27 (−0.29)	0.05 (−0.09)
Mini-Mental State Examination	0.09 (0.04)	−0.08 (−0.04)	0.33 (0.26)
Sleep tests			
Total sleep time (total sleep time)	−0.07 (−0.07)	0.05 (0.02)	−0.02 (0.02)
Sleep efficiency	0.03 (0.05)	0.11 (0.07)	−0.01 (−0.10)
N1 stage (% of total sleep time)	−0.18 (−0.20)	−0.00 (0.05)	−0.55 (−0.63)
N2 stage (%of total sleep time)	−0.06 (−0.06)	−0.34 (−0.33)	−0.02 (−0.12)
N3 stage (% of total sleep time)	−0.04 (−0.12)	−0.09 (−0.09)	0.20 (0.15)
REM sleep (% of total sleep time)	−0.14 (−0.10)	0.14 (0.12)	−0.01 (0.12)
REM sleep without atonia (% of REM sleep time)	−0.49** (−0.45*)	−0.50* (−0.50*)	−0.04 (−0.08)

Correlation corresponds to the R value. Results corrected for age and gender are reported into brackets. N1 stage = duration of stage 1 sleep divided by total sleep time; N2 stage = duration of stage 2 sleep divided by total sleep time; N3 + 4 stage = duration of stages 3 + 4 sleep divided by total sleep time; REM sleep = duration of REM sleep divided by total sleep time; REM sleep without atonia = duration of REM sleep without atonia divided by the total duration of REM sleep. *$P < 0.05$, **P-value < 0.005.

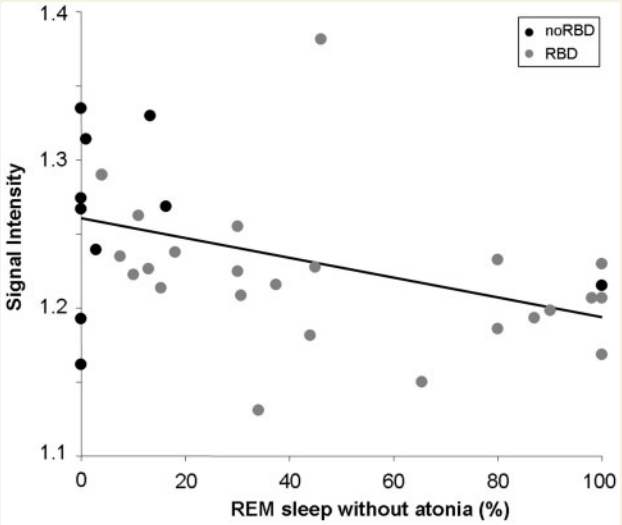

Figure 4 Correlation between the percentage of REM sleep without atonia and signal intensity in the locus area in the entire patient group. Signal intensity: normalized signal intensity in the locus area, black circles/noRBD = patients without RBD, grey circles = patients with RBD.

motor pathway that causes inhibition of spinal motor neurons (Lu *et al*., 2006; Boeve *et al*., 2007), but this remained to be demonstrated in patients with Parkinson's disease. Here, we provide, for the first time, direct evidence linking the locus coeruleus/subcoeruleus with atonia during REM sleep in humans.

The association of RBD with Parkinsonism, synucleinopathy and Lewy body pathology relies on strong evidence (Boeve *et al*., 2007). RBD has frequently been reported in association with idiopathic and genetic Parkinson's disease, dementia with Lewy bodies, and multiple system atrophy and less often with progressive supranuclear palsy (Boeve *et al*., 2007). In idiopathic Parkinson's disease, the temporal sequence of synuclein pathology has been proposed in a staging system that begins in the medulla and ascends towards more rostral structures including the locus coeruleus/subcoeruleus complex (Braak *et al*., 2004; Postuma *et al*., 2006). Dysfunction of the locus subcoeruleus is therefore considered as the plausible cause of REM sleep without atonia in patients with Parkinson's disease with RBD. In line with this hypothesis, signal intensities in the locus coeruleus/subcoeruleus area were decreased and correlated with the percentage of REM sleep without atonia in patients with RBD but not without RBD. In addition, more widespread abnormalities were observed using diffusion imaging in line with Braak's staging hypothesis. The temporal sequence of damage proposed by Braak would explain why RBD precedes motor signs in many patients with Parkinson's disease. However, this temporal sequence of synuclein deposition has also been questioned (Burke *et al*., 2008) as the occurrence of RBD does not always precede parkinsonism, an observation that is supported by current findings in patients without RBD. Together these results suggest that only patients with sufficient degeneration in this structure express RBD. There was some overlap in signal intensities in the locus coeruleus/subcoeruleus area between patients with and without RBD suggesting that some patients in the latter group presented mild degenerative changes in this region. This is also suggested by the lack of significant difference between the two groups of patients in the brainstem in the voxel-based analysis in agreement with a recent study (Ford *et al*., 2013). It is possible that patients without RBD presented mild signs of REM sleep dysfunction. First, we used a threshold of 30% of REM sleep without atonia (plus a history of dream enactment) to classify patients as RBD-positive based on a previous study (Gagnon *et al*., 2002), with some overlap between patients with and without clinical RBD. Second, complex movements may be absent during a single overnight monitoring, and clinical history of RBD may fluctuate over time (Lavault *et al*., 2010). Third, the abnormalities detected in the locus coeruleus/subcoeruleus area in patients without RBD may indicate subthreshold abnormalities that may be 'presymptomatic' to the occurrence of RBD. In addition, the amount of REM sleep without atonia predicts the risk of

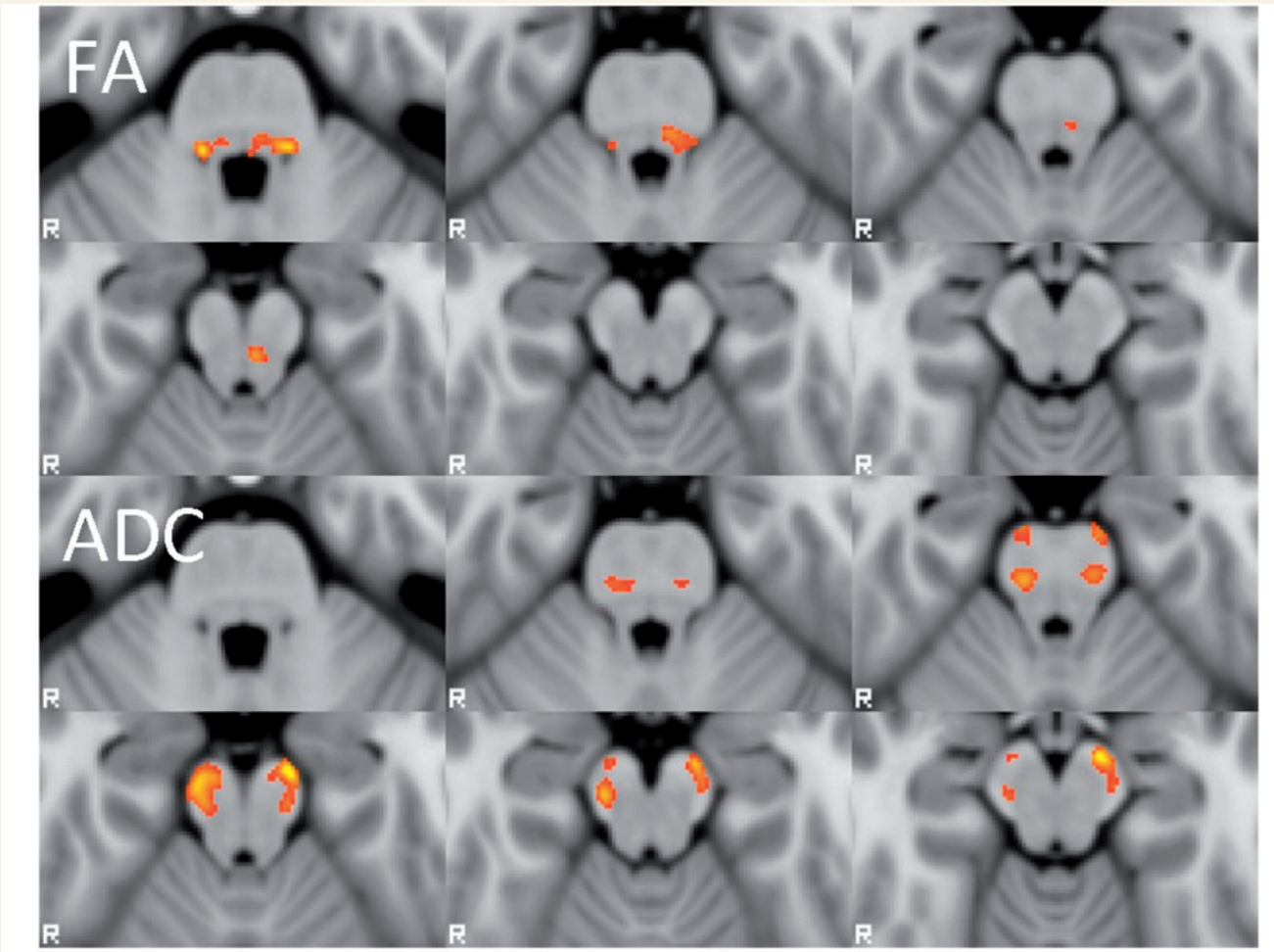

Figure 5 Statistical parametric maps of the diffusion analysis superimposed onto a normalized 3D T_1-weighted MRI scan of a healthy volunteer in the axial plane showing areas of significant increase in fractional anisotropy (FA) (*top*) and apparent diffusion coefficient (ADC) values (*bottom*) in patients with RBD as compared with healthy volunteers (colour code: orange to yellow). Maps are thresholded at $P < 0.001$ uncorrected. Clusters are significant at $P < 0.05$ corrected for multiple comparisons in the right hemisphere for fractional anisotropy and the left hemisphere for apparent diffusion coefficient and uncorrected in the opposite hemispheres.

converting rapidly to Parkinson's disease in idiopathic RBD (Postuma *et al*., 2009). Further study with refinement of the technique and longitudinal follow-up of patients will improve the neuroanatomical correlations and help determine whether imaging changes in the locus area are early markers that predict the occurrence of Parkinson's disease.

The locus subcoeruleus is part of catecholaminergic cell populations of the midbrain and pontine tegmentum. Neuromelanin is a pigment produced in catecholaminergic neurons. Neuromelanin-containing neurons are present in the pars compacta of the substantia nigra and the locus coeruleus/subcoeruleus complex (Bazelon *et al*., 1967; Zecca *et al*., 2003). Both the locus coeruleus and the subcoeruleus contain pigmented cells (Baker *et al*., 1989). Histological studies in humans without evidence of neurological diseases have shown that cells containing neuromelanin pigment were similar in number to tyrosine hydroxylase immunoreactive cells and were thus a good estimate of catecholamine cells (Baker *et al*., 1989). The locus coeruleus contains 50–60 000 cells with neuromelanin and the locus subcoeruleus ~6000 cells. In the midbrain, cells in the locus coeruleus are dispersed in the ventrolateral region of the central grey matter, medial to the mesencephalic tract of the trigeminal nerve. From this level, cells are found caudally from the nucleus in a ventrolateral direction and enter the region of the locus subcoeruleus (Baker *et al*., 1989).

Neuromelanin can be imaged using MRI. Melanin-sensitive techniques use the paramagnetic T_1-shortening effects of neuromelanin when combined with metals such as iron and copper (Enochs *et al*., 1997). The coeruleus/subcoeruleus area presents high intensity in spin echo T_1-weighted MRI images (Sasaki *et al*., 2006; Shibata *et al*., 2006; Keren *et al*., 2009). The spatial map of the human coeruleus/subcoeruleus complex that was obtained using MRI (Keren *et al*., 2009) closely resembled the 3D reconstructions of the structure obtained using serial histological sections of pigmented (German *et al*., 1988) or tyrosine hydroxylase immunostained cells (Baker *et al*., 1989). In addition, the distribution of the area of high signal intensity tightly correlated with the density of cells in the locus coeruleus complex reported in a post-mortem study (German *et al*., 1988), providing

convincing evidence that this area of increased signal is an accurate marker of the number of cells in the locus (Keren *et al*., 2009). Our results are in line with these studies. However, using this technique and given the small size of the structure, accurate delineation of the locus subcoeruleus from the locus coeruleus was not possible and separate analysis of the two structures was not performed. Therefore signal changes observed in the present study originate from both structures together.

We found a small left/right asymmetry in healthy volunteers as well as in patients. The reason for this asymmetry is not known as post-mortem studies reported that the distribution of the pigmented cells was largely symmetrical (German *et al*., 1988; Baker *et al*., 1989; Chan-Palay and Asan, 1989*a*, *b*; Ohm *et al*., 1997). In contrast, imaging studies reported some degree of asymmetry in the location or the variance of the peak signal intensity that may be related to methodological issues such as the difficulty of automated segmentation of the locus coeruleus/subcoeruleus complex because of its amorphous structure and varying signal intensity across subjects, and of signal inhomogeneity across the image particularly when using multi-channel coils.

Patients showed fractional anisotropy and apparent diffusion coefficient changes in areas of the brainstem, suggesting the presence of extranigral pathology in agreement with Braak's staging hypothesis (Braak *et al*., 2004; Postuma *et al*., 2006). This observation is also in line with the observation of fractional anisotropy and apparent diffusion coefficient changes in the brainstem of patients with idiopathic RBD, a condition associated with increased risk of developing Parkinson's disease (Scherfler *et al*., 2010). In contrast to this study, which reported decreased fractional anisotropy in the tegmentum of the midbrain and pons, fractional anisotropy was increased in the present study. Diffusion changes are thought to correlate to neuronal and myelin damage (Le Bihan and Johansen-Berg, 2011). Anisotropy describes the spatial variations of water molecular displacements and relates to the presence of oriented structures such as axons in fibre bundles. Factors such as membrane, myelin, longitudinal filaments and cytoskeleton contribute to anisotropy. In pathological conditions, anisotropy most often decreases as a result of fibre tract damage but may also increase in some instances (Delmaire *et al*., 2009; Douaud *et al*., 2009). The origin of increased anisotropy is not known but may be the result of the specific degeneration of one fibre tract in areas of fibre crossing (Douaud *et al*., 2009), as is the case in the brainstem. The variability in diffusion changes may also reflect differences in the evolution of the disease process as idiopathic RBD is supposed to precede the occurrence of Parkinson's disease by many years or differences in brainstem compartments that are potentially damaged (white and/or grey matter). Alternatively, differences in image analysis methods and group sizes may contribute to explain opposite findings. A recent study reported non-significant fractional anisotropy increase in the pontine tegmentum in patients with Parkinson's disease and RBD compared with patients without RBD (Ford *et al*., 2013). This observation is in line with the present findings as significant changes were not observed when both groups were compared directly but only when RBD patients were compared with healthy subjects. Other differences in this study include the diagnosis of RBD, which was based on questionnaire data with no video-polysomnographic recordings, and no control group. No correlations between diffusion and clinical variables were evidenced in the present study confirming that brain correlates of sleep disorders in patients with Parkinson's disease were more specifically depicted using neuromelanin-sensitive than diffusion imaging.

In summary using neuromelanin-sensitive MRI techniques and careful clinical evaluation combined with sleep and video monitoring, we found clear evidence that the locus coeruleus/subcoeruleus complex is involved in the pathophysiology of RBD and the control of atonia during REM sleep. This technique may be used in longitudinal studies as an early marker of non-dopaminergic Parkinson's disease pathology to predict the occurrence of Parkinson's disease. Refinement of the technique may help distinguish the locus coeruleus and subcoeruleus.

Acknowledgements

We thank Sebastien Bourret for his helpful comments.

Funding

The work was supported by Agence Nationale de la Recherche (ANRMNP 2009, Nucleipark), DHOS-Inserm (2010, Nucleipark), France Parkinson (2008), Ecole Neuroscience de Paris, 'Investissements d'avenir' [grant number ANR-10-IAIHU-06], Institut Fédératif de Recherche 49 (IFR 49).

References

Arnulf I. REM sleep behavior disorder: motor manifestations and pathophysiology. Mov Disord 2012; 27: 677–89.

Arnulf I, Bonnet AM, Damier P, Bejjani BP, Seilhean D, Derenne JP, et al. Hallucinations, REM sleep, and Parkinson's disease: a medical hypothesis. Neurology 2000; 55: 281–8.

Ashburner J, Friston KJ. Unified segmentation. Neuroimage 2005; 26: 839–51.

Avants BB, Epstein CL, Grossman M, Gee JC. Symmetric diffeomorphic image registration with cross-correlation: evaluating automated labeling of elderly and neurodegenerative brain. Med Image Anal 2008; 12: 26–41.

Baker KG, Tork I, Hornung JP, Halasz P. The human locus coeruleus complex: an immunohistochemical and three dimensional reconstruction study. Exp Brain Res 1989; 77: 257–70.

Bazelon M, Fenichel GM, Randall J. Studies on neuromelanin. I. A melanin system in the human adult brainstem. Neurology 1967; 17: 512–9.

Boeve BF, Silber MH, Saper CB, Ferman TJ, Dickson DW, Parisi JE, et al. Pathophysiology of REM sleep behaviour disorder and relevance to neurodegenerative disease. Brain 2007; 130: 2770–88.

Boissard R, Fort P, Gervasoni D, Barbagli B, Luppi PH. Localization of the GABAergic and non-GABAergic neurons projecting to the sublaterodorsal nucleus and potentially gating paradoxical sleep onset. Eur J Neurosci 2003; 18: 1627–39.

Boissard R, Gervasoni D, Schmidt MH, Barbagli B, Fort P, Luppi PH. The rat ponto-medullary network responsible for paradoxical sleep onset and maintenance: a combined microinjection and functional neuroanatomical study. Eur J Neurosci 2002; 16: 1959–73.

Braak H, Del Tredici K, Rub U, de Vos RA, Jansen Steur EN, Braak E. Staging of brain pathology related to sporadic Parkinson's disease. Neurobiol Aging 2003; 24: 197–211.

Braak H, Ghebremedhin E, Rub U, Bratzke H, Del Tredici K. Stages in the development of Parkinson's disease-related pathology. Cell Tissue Res 2004; 318: 121–34.

Burke RE, Dauer WT, Vonsattel JP. A critical evaluation of the Braak staging scheme for Parkinson's disease. Ann Neurol 2008; 64: 485–91.

Chan-Palay V, Asan E. Alterations in catecholamine neurons of the locus coeruleus in senile dementia of the Alzheimer type and in Parkinson's disease with and without dementia and depression. J Comp Neurol 1989a; 287: 373–92.

Chan-Palay V, Asan E. Quantitation of catecholamine neurons in the locus coeruleus in human brains of normal young and older adults and in depression. J Comp Neurol 1989b; 287: 357–72.

Comella CL, Nardine TM, Diederich NJ, Stebbins GT. Sleep-related violence, injury, and REM sleep behavior disorder in Parkinson's disease. Neurology 1998; 51: 526–9.

De Cock VC, Debs R, Oudiette D, Leu S, Radji F, Tiberge M, et al. The improvement of movement and speech during rapid eye movement sleep behaviour disorder in multiple system atrophy. Brain 2011; 134: 856–62.

De Cock VC, Vidailhet M, Leu S, Texeira A, Apartis E, Elbaz A, et al. Restoration of normal motor control in Parkinson's disease during REM sleep. Brain 2007; 130: 450–6.

Delmaire C, Vidailhet M, Wassermann D, Descoteaux M, Valabregue R, Bourdain F, et al. Diffusion abnormalities in the primary sensorimotor pathways in writer's cramp. Arch Neurol 2009; 66: 502–8.

Douaud G, Behrens TE, Poupon C, Cointepas Y, Jbabdi S, Gaura V, et al. *In vivo* evidence for the selective subcortical degeneration in Huntington's disease. Neuroimage 2009; 46: 958–66.

Duclap D, Lebois A, Schmitt B, Riff O, Guevara P, Marrakchi-Kacem L, et al. Connectomist-2.0: a novel diffusion analysis toolbox for BrainVISA. European Society for Magnetic Resonance in Medicine and Biology. Lisbon, Portugal: Springer; 2012.

Enochs WS, Petherick P, Bogdanova A, Mohr U, Weissleder R. Paramagnetic metal scavenging by melanin: MR imaging. Radiology 1997; 204: 417–23.

Folstein MF, Folstein SE, McHugh PR. "Mini-mental state". A practical method for grading the cognitive state of patients for the clinician. J Psychiatr Res 1975; 12: 189–98.

Fonov V, Evans AC, Botteron K, Almli CR, McKinstry RC, Collins DL. Unbiased average age-appropriate atlases for pediatric studies. Neuroimage 2011; 54: 313–27.

Ford AH, Duncan GW, Firbank MJ, Yarnall AJ, Khoo TK, Burn DJ, et al. Rapid eye movement sleep behavior disorder in Parkinson's disease: magnetic resonance imaging study. Mov Disord 2013, Feb 28. doi:10.1002/mds.25367.

Gagnon JF, Bedard MA, Fantini ML, Petit D, Panisset M, Rompre S, et al. REM sleep behavior disorder and REM sleep without atonia in Parkinson's disease. Neurology 2002; 59: 585–9.

German DC, Walker BS, Manaye K, Smith WK, Woodward DJ, North AJ. The human locus coeruleus: computer reconstruction of cellular distribution. J Neurosci 1988; 8: 1776–88.

Iber C, Ancoli-Israel S, Chesson AL, Quan SF. The AASM Manual for the Scoring of Sleep and Associated Events: Rules, Terminology and Technical Specifications. 1st edn. Westchester, IL: American Academy of Sleep Medicine; 2007.

Iranzo A, Aparicio J. A lesson from anatomy: focal brain lesions causing REM sleep behavior disorder. Sleep Med 2009; 10: 9–12.

Iranzo A, Molinuevo JL, Santamaria J, Serradell M, Marti MJ, Valldeoriola F, et al. Rapid-eye-movement sleep behaviour disorder as an early marker for a neurodegenerative disorder: a descriptive study. Lancet Neurol 2006; 5: 572–7.

Jenkinson M, Beckmann CF, Behrens TE, Woolrich MW, Smith SM. Fsl. Neuroimage 2011; 62: 782–90.

Keren NI, Lozar CT, Harris KC, Morgan PS, Eckert MA. *In vivo* mapping of the human locus coeruleus. Neuroimage 2009; 47: 1261–7.

Kimura K, Tachibana N, Kohyama J, Otsuka Y, Fukazawa S, Waki R. A discrete pontine ischemic lesion could cause REM sleep behavior disorder. Neurology 2000; 55: 894–5.

Lavault S, Leu-Semenescu S, Tezenas du Montcel S, Cochen de Cock V, Vidailhet M, Arnulf I. Does clinical rapid eye movement behavior disorder predict worse outcomes in Parkinson's disease? J Neurol 2010; 257: 1154–9.

Le Bihan D, Johansen-Berg H. Diffusion MRI at 25: exploring brain tissue structure and function. Neuroimage 2011; 61: 324–41.

Limousin N, Dehais C, Gout O, Heran F, Oudiette D, Arnulf I. A brainstem inflammatory lesion causing REM sleep behavior disorder and sleepwalking (parasomnia overlap disorder). Sleep Med 2009; 10: 1059–62.

Lu J, Sherman D, Devor M, Saper CB. A putative flip-flop switch for control of REM sleep. Nature 2006; 441: 589–94.

Luppi PH, Clement O, Sapin E, Gervasoni D, Peyron C, Leger L, et al. The neuronal network responsible for paradoxical sleep and its dysfunctions causing narcolepsy and rapid eye movement (REM) behavior disorder. Sleep Med Rev 2010; 15: 153–63.

Manjon JV, Coupe P, Marti-Bonmati L, Collins DL, Robles M. Adaptive non-local means denoising of MR images with spatially varying noise levels. J Magn Reson Imaging 2010; 31: 192–203.

Montplaisir J, Gagnon JF, Fantini ML, Postuma RB, Dauvilliers Y, Desautels A, et al. Polysomnographic diagnosis of idiopathic REM sleep behavior disorder. Mov Disord 2010; 25: 2044–51.

Ohm TG, Busch C, Bohl J. Unbiased estimation of neuronal numbers in the human nucleus coeruleus during aging. Neurobiol Aging 1997; 18: 393–9.

Postuma RB, Gagnon JF, Vendette M, Fantini ML, Massicotte-Marquez J, Montplaisir J. Quantifying the risk of neurodegenerative disease in idiopathic REM sleep behavior disorder. Neurology 2009; 72: 1296–300.

Postuma RB, Lang AE, Massicotte-Marquez J, Montplaisir J. Potential early markers of Parkinson disease in idiopathic REM sleep behavior disorder. Neurology 2006; 66: 845–51.

Provini F, Vetrugno R, Pastorelli F, Lombardi C, Plazzi G, Marliani AF, et al. Status dissociatus after surgery for tegmental ponto-mesencephalic cavernoma: a state-dependent disorder of motor control during sleep. Mov Disord 2004; 19: 719–23.

Sasaki M, Shibata E, Tohyama K, Takahashi J, Otsuka K, Tsuchiya K, et al. Neuromelanin magnetic resonance imaging of locus ceruleus and substantia nigra in Parkinson's disease. Neuroreport 2006; 17: 1215–8.

Sastre JP, Jouvet M. Oneiric behavior in cats. Physiol Behav 1979; 22: 979–89.

Schenck CH, Mahowald MW. REM sleep behavior disorder: clinical, developmental, and neuroscience perspectives 16 years after its formal identification in SLEEP. Sleep 2002; 25: 120–38.

Scherfler C, Frauscher B, Schocke M, Iranzo A, Gschliesser V, Seppi K, et al. White and gray matter abnormalities in idiopathic rapid eye movement sleep behavior disorder: a diffusion-tensor imaging and voxel-based morphometry study. Ann Neurol 2010; 69: 400–7.

Shibata E, Sasaki M, Tohyama K, Kanbara Y, Otsuka K, Ehara S, et al. Age-related changes in locus ceruleus on neuromelanin magnetic resonance imaging at 3 Tesla. Magn Reson Med Sci 2006; 5: 197–200.

Sled JG, Zijdenbos AP, Evans AC. A nonparametric method for automatic correction of intensity nonuniformity in MRI data. IEEE Trans Med Imaging 1998; 17: 87–97.

Tippmann-Peikert M, Boeve BF, Keegan BM. REM sleep behavior disorder initiated by acute brainstem multiple sclerosis. Neurology 2006; 66: 1277–9.

Tohka J, Zijdenbos A, Evans A. Fast and robust parameter estimation for statistical partial volume models in brain MRI. Neuroimage 2004; 23: 84–97.

Unger MM, Belke M, Menzler K, Heverhagen JT, Keil B, Stiasny-Kolster K, et al. Diffusion tensor imaging in idiopathic REM sleep behavior disorder reveals microstructural changes in the brainstem, substantia nigra, olfactory region, and other brain regions. Sleep 2010; 33: 767–73.

Zecca L, Zucca FA, Wilms H, Sulzer D. Neuromelanin of the substantia nigra: a neuronal black hole with protective and toxic characteristics. Trends Neurosci 2003; 26: 578–80.